

Robust Determination of the Pore-Space Morphology in Sedimentary Rocks

This approach to study the morphology (shapes and connectivity) of sedimentary-rock pore space is based on fundamental concepts of mathematical morphology. An efficient and stable algorithm is proposed that distinguishes between the pore bodies and pore throats and establishes their respective volumes and connectivity.

Introduction

Fluid transport through a permeable rock is determined by the void-space geometry and connectivity and the solid-surface/fluid chemistry. The ever-changing distribution of fluids in the pores of a gas- and oil-bearing rock must be understood to develop a successful hydrocarbon-recovery process. The process-dependent redistribution of reservoir fluids during production and injection determines how much of the initial hydrocarbons will be recovered and how much will be trapped. Although the length-scale of an oil field is measured in kilometers, the ultimate success of an oil- and gas-recovery scheme is the net result of countless displacement events at a scale measured in micrometers. Recent advances in microimaging of natural rocks, combined with advances in pore-network flow modeling, enable a better understanding of pore-level displacement mechanisms. It is possible to make credible predictions of the effects of the rock wettability and fluid properties on the relative permeabilities and capillary pressures, as well as on the trapped-oil and -gas saturations.

Imaging

A microscopic image of rock is a 3D array of cubic atoms or voxels. Each voxel is assigned a nonzero value if it is attributed to the pore space and zero otherwise. A group of neighboring voxels can make a loosely defined "pore throat" or a "pore body." In modeling, the pore throats control fluid flow, whereas the pore bodies provide fluid storage. Even at this level, rock description is approximate. First, the number and size of the voxels in an image are limited by the resolution and viewing angle of the imaging device. Second, the image itself is often an

interpretation of the reflection, absorption, attenuation, and diffraction patterns of electromagnetic waves. Each such interpretation is a solution of a series of inverse problems. The inversion errors are then combined with errors inevitably produced by assignments of the voxels that are part solid and part void space. The representativeness of a digital image, and the determination of minimum resolution necessary to image a given rock adequately, are issues yet to be appropriately addressed in the literature.

Many computer "skeletonization" algorithms are based on thinning methods, which remove the redundant elements of an image while preserving certain topological properties of the entire pore space. Tests of thinning algorithms on simple computer-generated images show that a refinement of the resolution can lead to less accurate results. A skeletonization method, based on a complete catalog of shape primitives for 2D and 3D objects, was developed. Characterizing the pore-space geometry without applying thinning algorithms was proposed. In particular, characterizing the skeleton as the set of centers of the maximal balls was used.

Pore-Body and Pore-Throat Detection Algorithm

A weak point of thinning algorithms is that once a voxel is deleted from the set, all information related to this voxel is lost, and the cumulative effect can distort the result. Processing images by parts is impossible because the result depends on which voxel is removed first when multiple choices exist.

This procedure does not remove voxels. Instead, the information is stored in an aggregate format. In the interior part, far enough from the boundary, the result of image analysis depends neither on the orientation of the image nor on the selection among the multiple choices of voxels to be removed.

At this stage, the algorithm does not produce a complete pore network ready for single-phase- or multiphase-flow simulations. However, it robustly characterizes the pore connectivity through a stick-and-ball representation.

*This article, written by Technology Editor Dennis Denney, contains highlights of paper SPE 84296, "Robust Determination of the Pore-Space Morphology in Sedimentary Rocks," by **Dmitry B. Silin**, SPE, Lawrence Berkeley Natl. Laboratory; **Guodong Jin**, SPE, U. of California, Berkeley; and **Tad W. Patzek**, SPE, U. of California, Berkeley/Lawrence Berkeley Natl. Laboratory, prepared for the 2003 SPE Annual Technical Conference and Exhibition, Denver, 5–8 October.*

Building Voxel Objects. A voxel object is one of the basic elements of this algorithm. It corresponds to a voxel in the image; therefore, it has three coordinates. Further, each voxel "knows" its maximal radius (i.e., the radius of the corresponding maximal ball). In addition, each voxel has two lists of pointers to other voxels. In all calculations, unit length is the linear size of one voxel.

First, the algorithm calculates the maximal-ball radius for each voxel. Starting from a zero-radius ball (i.e., the voxel itself), the radius of the ball is incremented by one step until the ball hits a solid-phase voxel. The algorithm complexity increases rapidly with refinement of the image resolution.

After all maximal balls are constructed, some are subsets of others. Both included balls and the corresponding voxels carry information about the pore space that is already stored in the including ball or balls. Therefore, the second step in the algorithm is removal of the included balls. To perform this operation, it is convenient to store all voxels in a sorted list, in which the sorting is by the maximal radius.

In this procedure, the set of centers of the voxels remaining in the list after removal of the included maximal balls is the skeleton of the pore space. The order in which these voxels are calculated does not matter. If a large image must be processed, it can be split into parts, each part can be analyzed separately, and the results can be merged into the skeleton of the whole pore space. Therefore, a computer with a mod-

est memory size can be used to process a large image.

Finding only the skeleton is not sufficient. To characterize the pore space, the “redundant ribs” corresponding to the corners and similar structures should be removed. The voxel objects already “know” the radii of their maximal balls. Note that the maximal radius decreases along a rib leading into a corner. Therefore, a hierarchy of the skeleton voxels needs to be established. If the maximal balls of two voxels overlap, the one with the larger radius is called master and the other is called slave. Thus, the third step of the algorithm is to search for the slaves of each voxel. For each current voxel, a domain in which potentially overlapping voxels can exist is determined from the radius of its maximal ball. Next, using the pointers provided for these locations by the reference table, the slave voxels are found. Then, the two lists of pointers for each voxel include pointers to the masters and slaves of this voxel, respectively.

After building the hierarchy, there are many voxels that are masters and slaves at the same time. To characterize the pore, only the voxel with the largest maximal ball is retained. This characterization is done through a four-step enhanced hierarchy procedure, the purpose of which is to retain only the largest master voxels. This procedure is detailed in the full-length paper.

It is natural to call the union of all maximal balls associated with the voxels connecting two given master voxels a pore throat. In the stick-and-ball diagram, a pore throat connecting two pore bodies is depicted as a straight-line segment connecting the centers of the balls associated with these pore bodies.

Algorithm Verification. To verify a physical model, numerical or analytical simulations should be compared with field or laboratory measurements. To verify a numerical algorithm, a test problem with a known analytical solution can be considered, and the numerical result compared with the exact one. In image analysis, verifying an algorithm is not straightforward. The test image must have sufficiently complicated geometry with internal openings and connections between them. Also, the image should be small and simple so that the results of computations will be transparent and verifiable.

To verify this algorithm, a computer-generated packing of equal spheres was used. The spheres are packed in layers. Every layer in which all spheres touch each other is sandwiched between two layers in which each sphere is tangential to four spheres from one layer below and four spheres from

one layer above (**Fig. 1a**). The whole pack is shown in Fig. 1b, and its porosity, if the stencil in Fig. 1a is applied indefinitely, is approximately 26%.

In some cases, the results can be reasonably good if the sphere pack is aligned with the coordinate axes, but the algorithm may fail in other situations. Therefore, to test the algorithm, the whole pack of spheres was rotated. Then, a part of the image cut by a cube was analyzed. The pore space of this part is shown in **Fig. 2**. **Fig. 3** shows the stick-and-ball diagram. No quantitative criterion of whether the pore-body and pore-throat shapes are detected correctly can be applied, and the shape analysis can be performed only visually.

It is difficult to specify the rigorous requirements for a “sufficient” resolution of a rock image. However, numerical experiments with images of the various computer-generated sphere packs show that for an adequate description of the pore space, the resolution should be at least one order of magnitude finer than the representative sphere radius.

Dimensionless Capillary Pressure

When the pore space is shared between two immiscible fluids in equilibrium, the wetting fluid occupies the corners of both large and small pores, while the nonwetting fluid occupies the central part of the invaded pores. An interface between these two fluids is a surface the curvature of which is determined by the capillary pressure. In reality, the fluid interfaces are not spherical; however, spheres can approximate them. The information about the maximal balls can be used to reconstruct a capillary pressure curve.

Information about the maximal-ball distribution enabled computing a dimensionless drainage-capillary-pressure curve, which simulates mercury injection. It was concluded that the calculated capillary pressure curve was a robust descriptor of the pore-space geometry, and it can be used to determine the quality of computer reconstruction of natural rocks. Also, an appropriate scaling of this curve should predict the capillary pressure of the rock on the basis of its 3D image. This scaling has not yet been developed because of a lack of appropriate experimental data. The authors observed that the nonwetting-phase breakthrough saturation during drainage has lit-

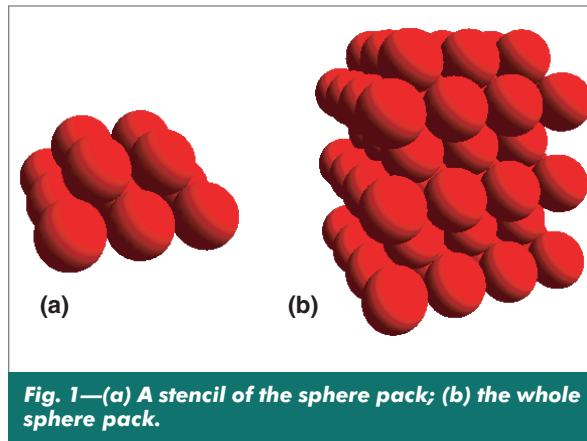


Fig. 1—(a) A stencil of the sphere pack; (b) the whole sphere pack.

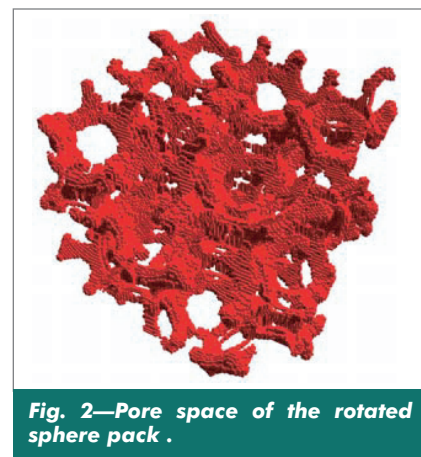


Fig. 2—Pore space of the rotated sphere pack .

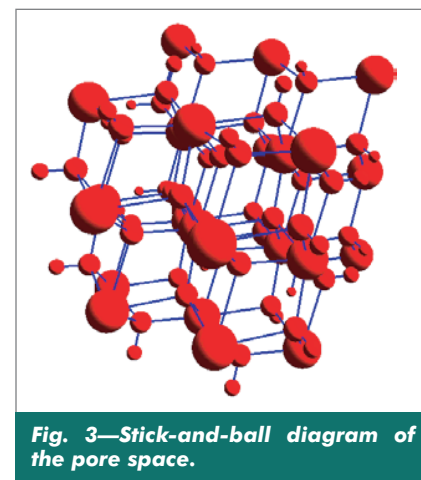


Fig. 3—Stick-and-ball diagram of the pore space.

tle relation to the sandstone porosity. Moreover, at least within the considered length scales, this breakthrough occurs at lower capillary pressures in larger sandstone samples. **JPT**

For a limited time, the full-length paper is available free to SPE members at www.spe.org/jpt. The paper has not been peer reviewed.